



Structural and Optical Properties of $\text{SiO}_x/\text{Au}/\text{SiO}_x$ Layer Films on the Effect of Rapid Thermal Annealing Process

Najwa Rosli¹, Keewah Chan², Saadah A. Rahman³, Ilyani Putri Jamal⁴, Zarina Aspanut^{5*}

¹⁻⁵ Low Dimensional Materials Research Centre, Department of Physics, University of Malaya, 50603, Kuala Lumpur, Malaysia y

Email: zarinaaspanut@um.edu.my

(Received July 2011; Published December 2011)

ABSTRACT

In this work, layered of silicon suboxide/gold/silicon suboxide ($\text{SiO}_x/\text{Au}/\text{SiO}_x$) films were prepared by using hot-wire plasma enhanced chemical vapor deposition (HW-PECVD) system. The films prepared underwent rapid thermal annealing (RTA) process for time periods of 100s, 500s and 700s at temperature of 800°C in vacuum. The effects of RTA on the structural and morphology from FE-SEM, Auger and XRD measurement of the films were studied. The surface plasmon resonance (SPR) effect exhibited by Au particles was obtained from the optical absorption spectra. SPR peaks were exhibited by films which annealed for long time duration. The band gap energy of the annealed samples was found to be in the range of 1.8 to 2.05 eV.

Key words: Silicon, Plasma Enhanced Chemical Vapour Deposition (PECVD), FE-SEM, XRD

INTRODUCTION

Nanostructured material from composite of metal-dielectric film has a great interest in modern nanotechnology revolution due to their interesting structural, optical and electrical properties. Potential applications of this material include optoelectronic, sensors, anti-reflection coating for solar cell, photonic device and ultrafast optical switches (Zhuo, Li, Teng, & Yang, 2010). Nanocomposite films of this kind such as Au/ZnO, Ag/SiO₂, Au/SiO₂ (Pal et al., 2001), ZnO/SiO₂ (Scalisi, Compagnini, D'Urso, & Puglisi, 2004) and Au/Al₂O₃ (Garcia-Serrano, Galindo, & Pal, 2004) have been studied by many researchers in the last decade. In addition, nanocomposites films based on Au nanoparticles (AuNPs) embedded in various dielectric matrix, have been extensively studied as they demonstrate high structural stability, are easy to prepare and have novel optical properties (Ko, Mizuhata, Kajinami, & Deki, 2005; Xu & Perry, 2007) which are suitable for photocatalysts and sensor materials applications (Jung, Yoon, Koshizaki, & Kwon, 2008). The size of Au particle plays an important role in these composites to tune the properties for the exact technical need as reported by many researchers (Armelaio et al., 2004; Fu, Cai, Kan, Li, & Zhang, 2003; Su et al., 2008). A number of

techniques such as RF magnetron sputtering, ion implantation and PECVD etc. (Ruffino et al., 2007; Sangpour, Akhavan, Moshfegh, & Roozbehi, 2007; Tsuji et al., 2006) have been used to deposit metal-dielectric films. PECVD techniques have been shown to provide better coating uniformity and flexibility in selecting of deposition conditions. Recently, rapid thermal annealing (RTA) has been commonly used compared to the conventional thermal annealing process in order to improve film properties since the ultra-fast annealing time does not affect the device properties when the film is used in devices. Thus, many recent reported works on the effect of annealing on thermally sputtered oxide or sputter oxide films using RTA process can be obtained (Choi, Choo, & Lu, 1996). In these works, much attention has been focused on the RTA process on SiO₂ layers to improve the quality and reliability of SiO₂ films. However, the annealing process strongly depends on the process parameters which include temperature, ambient atmosphere and annealing time that can affect final properties of the film after RTA (Choi et al., 1996; Severi et al., 1992; Yu & Lu, 2000). Therefore, in this study, $\text{SiO}_x/\text{Au}/\text{SiO}_x$ films were prepared on Si (111) and quartz by using HW-PECVD. These films then undergo rapid thermal annealing process in vacuum condition at fixed temperature of 800°C and the effects of annealing time (100s,

500s and 700s) on the structural and optical properties of the films were investigated. The surface morphology of films was examined by field emission scanning electron microscope and surface profiler while the optical absorption was measured by UV-Vis-NIR spectrometer.

EXPERIMENTAL METHOD

Silicon suboxide/gold/silicon suboxide ($\text{SiO}_x/\text{Au}/\text{SiO}_x$) films were prepared using Plasma Enhanced Chemical Vapor Deposition (PECVD) system assisted with hot wire evaporation technique on the p-type (111) crystal silicon and quartz substrates. A piece of Au wire, 4 mm in length and 1 mm in diameter was placed on the tungsten filament at a distance of 350 mm above the substrates. The flow rate of nitrous oxide (N_2O) and silane (SiH_4) gases were fixed at 60 sscm and 2 sccm respectively. The rf power, deposition pressure and deposition time were fixed at 100W, 1.0 mbar and 1 hour respectively throughout the entire deposition process while substrate and filament temperatures were kept at 300°C and 1900°C respectively during the Au evaporation process. The first layer of SiO_x was introducing on the top of the substrates by dissociation of SiH_4 and N_2O gases. Thin layer of Au then was evaporating on the top of the SiO_x by using hot-wire techniques. After Au evaporation process, the dissociation of SiH_4 and N_2O gases were done again to fabricate again to form SiO_x layer on the top of the film. The annealing process on the films was carried out using a rapid thermal system at fixed temperature of 800°C in vacuum condition. Four different sets of films with their annealing time fixed at 100s, 300s, 500s and 700s were studied

The crystallinity of samples were characterized using a Siemens D5000 X-Ray diffractometer with $\text{Cu-K}\alpha$ radiation ($\lambda = 1.54056 \text{ \AA}$). The XRD spectra were taken at a grazing angle of 2°. The size, shape and distribution of Au particles on the SiO_x surface were investigated using field emission scanning electron microscope (FESEM) with model of FEI Quanta 200. The optical spectrum of transmittance and reflection of the samples were characterized using a JASCO V570 UV-VIS-NIR spectrophotometer.

RESULT AND DISCUSSION

XRD spectra for $\text{SiO}_x/\text{Au}/\text{SiO}_x$ films annealed by RTA process at temperature of 800°C using different annealing times are presented in Fig. 1. These spectra showed only one broad of Au (111) diffraction peak for the as-prepared film. The annealed films shows four Au diffraction peaks at 38.2°, 44.4°, 64.6° and 77.5° which corresponded to Au (111), Au (200), Au (220) and Au (311) crystalline planes respectively. It was observed that the SiO_x films are amorphous in structure as no SiO_x crystalline peak was observed. Furthermore, increase in the annealing time resulted in an increase in intensity and sharpness of the Au (111) diffraction peaks as shown in Fig. 1. Thus, this clearly indicated that the crystallinity of the Au was enhanced with increase in the annealing time. The estimated average of Au crystallite size was obtained by using Scherrer's equation (Chan, Aspanut, Goh, Muhamad, & Rahman, 2011). As observed from the Table 1, the estimated average of Au crystallite size was found to be in the range of about 9.6 nm to 26.3 nm. It was observed that the crystallite size determined from the Au

(111) orientation plane increased with increase in annealing time. The crystallite size determined from the Au (200), Au (220) and Au (311) orientation planes only showed a slightly decrease. This indicates that this orientation plane was stable and was not much affected by the annealing time.

		Crystallite Size (nm)			
		Au (111)	Au (200)	Au (220)	Au (311)
As prepared samples		9.6	-	-	-
Different annealing time	100s	22.9	21.9	23.7	25.4
	500s	26.2	17.8	24.8	28.4
	700s	26.3	18.9	22.8	20.3

Table.1 show XRD spectra and the estimated average of Au crystallite sizes respectively of as prepared $\text{SiO}_x/\text{Au}/\text{SiO}_x$ films and annealed $\text{SiO}_x/\text{Au}/\text{SiO}_x$ films at different annealing time of RTA process at temperature of 800°C.

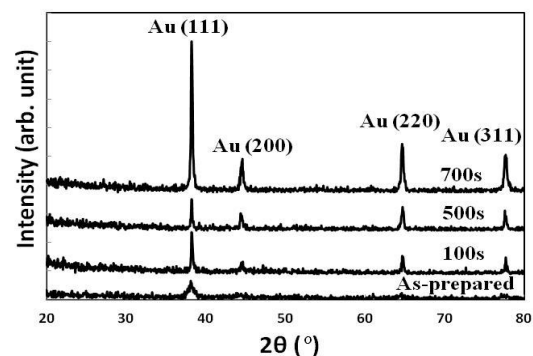


Fig.1 XRD spectra and the estimated average of Au crystallite sizes respectively of as prepared $\text{SiO}_x/\text{Au}/\text{SiO}_x$ films and annealed $\text{SiO}_x/\text{Au}/\text{SiO}_x$ films at different annealing time of RTA process at temperature of 800°C.

The absorption spectra of the as-prepared and annealed $\text{SiO}_x/\text{Au}/\text{SiO}_x$ films annealed at different annealing times using RTA process at temperature of 800°C are presented in Fig. 2. The absorption spectra, α can be evaluated from the relation of transmission and absorption spectra using the expression below:

$$T = (1 - R)e^{-\alpha d} \quad \text{which} \quad \alpha = 1/d \ln(1 - R/T) \quad (1)$$

where T, R and d are the transmittance, reflectance and the thickness of the films determine from the depth profiling respectively. As observed from the Fig. 2 in the UV region, the peaks at 380 nm and 386 nm were observed for the as-prepared film and the film annealed for 100s respectively. Both peaks corresponded to the $5d \rightarrow 6sp$ interbands transition of AuNPs. This is due the transition of electrons from the occupied d-level state to an empty state in the conduction band above the Fermi level like in a noble metal (Balamurugan & Maruyama, 2007).

Whereas, in the Vis region, the film annealed for 500s and 700s exhibited Surface Plasmon Resonance (SPR) peaks at 546 nm and 610 nm respectively indicating a blue-shift in this SPR peak with increase in annealing time. These SPR peak shifted towards lower wavelength (higher energy) along with the increase in intensity and sharpness of this peak when the annealing time was increased to 700s. This can be attributed to the change in shape and increase in size of the

Au particles. On the other hand, the interband transitions peaks shifted towards the higher wavelength side (lower energy) when annealed film for 100s.

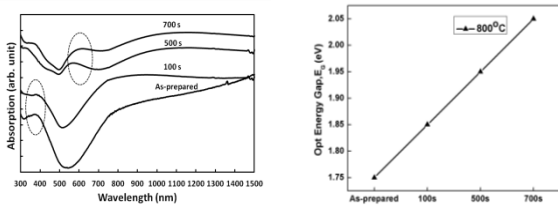


Fig. 2 and 3 Absorption spectra and Optical Energy Gap of as-prepared and annealed SiO_x/Au/SiO_x films at different annealing time of RTA process at temperature of 800°C.

The interband transitions were greatly suppressed when annealed at 500s which could be due to the change in the structure of the nanoparticles. Fig. 3 presents the variation of

optical energy gap of the as-prepared and annealed SiO_x/Au/SiO_x films at different annealing time. The optical energy gap of the film can be evaluated by applying the absorption coefficient based on Tauc relation (Balamurugan & Maruyama, 2007).

As indicated in Fig 3, optical energy gap of the films was directly proportional to the increase annealing time. It is observed that the optical energy gap, E_g of the as prepared and the annealed films were found in the range of 1.75 to 2.05 eV as shown in Fig.3. The increase in the intensity of SPR peaks induced by the Au particles when films annealed at 500s and 700s may related to increase in the energy gaps.

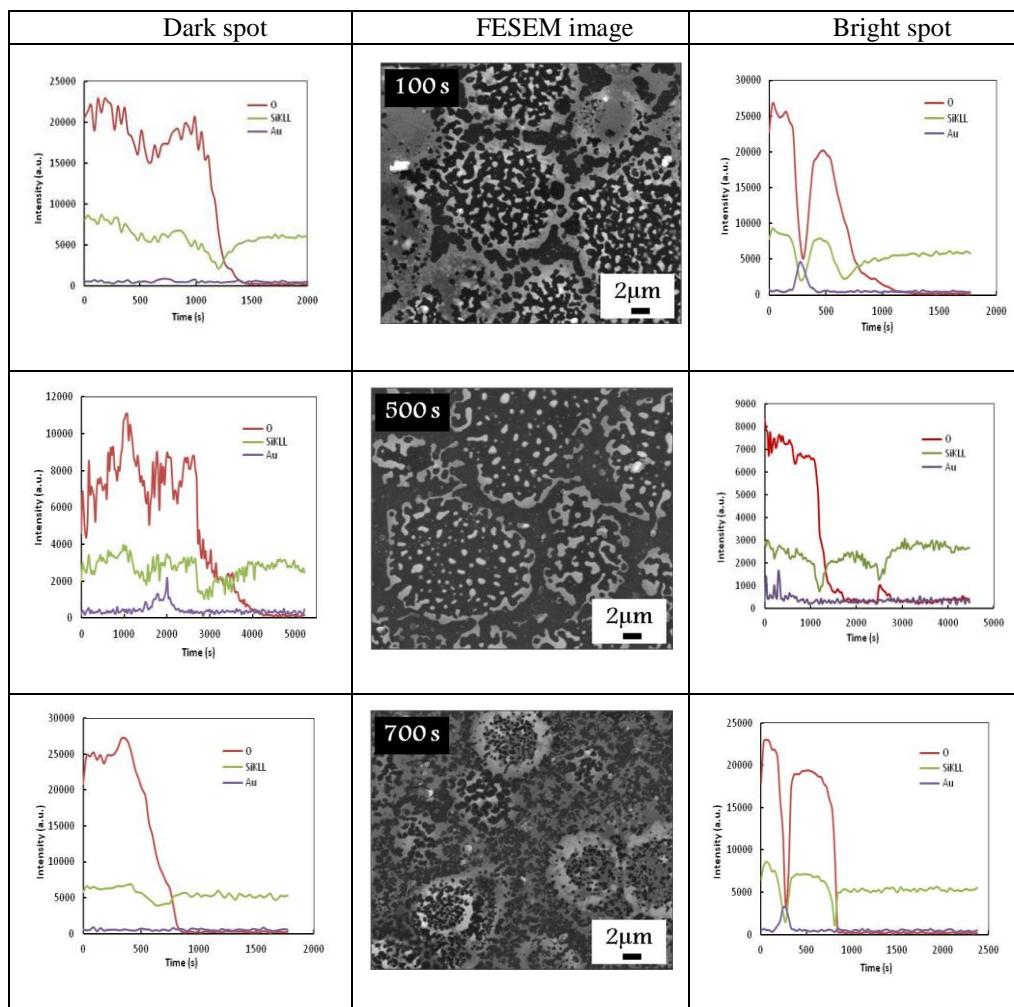


Fig. 4. FESEM images and Auger spectra (dark and bright spot) of annealed SiO_x/Au/SiO_x films of RTA process at temperature of 800°C with different annealing time.

FESEM images and Auger spectra analyzed on the dark and bright spots of annealed SiO_x/Au/SiO_x films at different annealing time are presented in Fig. 4. As observed from the FESEM image, it clearly shows that islands of Au nanoparticles increases and formed spherical shapes when the annealing time was increased from 100s to 700s. The transformation of the structure in the FESEM images can be related to elemental composition in these spots through the AES spectra. For the film annealed at 100s and 700s, it was

observes that SiO_x is more dominant on the dark spots in the film due to the movement of oxygen towards the surface as shown by the spectra. Moreover, the presence of high concentration of oxygen and silicon atoms moving towards the surface and absence of Au atoms as shown by the intensity of the AES profiles of these atoms in the dark spot region of both annealed films indicated that these dark spots were dominant SiO_x region. However, a small Au peak was observed at the centre of depth profile on the dark spot of the

500s annealed film. This indicated that the Au atoms in the layer sandwiched in between the SiO_x layers stated to diffuse towards the centre in the dark spots when annealed at 500 s. This also suggested that Au atoms started to agglomerate when annealed for 500s. The layered structure of SiO_x/Au/SiO_x film was still clearly observed at the bright spots of the film which annealed at 100s. When the annealing time of the film was increased to 500s, movements of oxygen and Au towards the surface of the film were observed on the bright spots of the film indicating the agglomerations of the Au nanoparticles started at this annealing temperature. However, very well defined layer of SiO_x/Au/SiO_x film was observed again in the film annealed at 700s indicating that the agglomeration was blocked resulting in the restructuring of the film. From other reported work (Chan et al., 2011) agglomeration of Au particles can be effectively blocked when either the oxygen or silicon content in SiO_x film is dominant. As the dark spots on the film showed that the oxygen content was high in this annealed film, thus supporting that the agglomeration of Au atoms in the

SiO_x/Au/SiO_x film was blocked causing the layers to be restructured.

CONCLUSION

The effects of rapid thermal annealing at different annealing time of SiO_x/Au/SiO_x films on the structural and optical properties have been studied. Crystallinity and the crystallite size of Au was enhanced when the annealing time of the films was increased. The absorption spectra revealed two predominant absorption peaks in the UV and VIS regions which corresponded to the interband transition and SPR peaks. The interband transition in the AuNP from the 5*d* to the 6*sp* was significant in the as-prepared and films annealed for 100s whereas longer annealing times of 500s and 700s resulted in changes in the shape and sizes of Au nanoparticles as indicated by the blue shift of SPR peaks. The interband transition of AuNP was suppressed as a result the change in size and shape of the nanoparticles in the films.

REFERENCES

- Armelao, L., Barreca, D., Bottaro, G., Gasparotto, A., Tondello, E., Ferroni, M., & Polizzi, S. (2004). Au/TiO₂ nanosystems: a combined RF-Sputtering/Sol-Gel approach. *Chemistry of materials*, 16(17), 3331-3338.
- Balamurugan, B., & Maruyama, T. (2007). Size-modified d bands and associated interband absorption of Ag nanoparticles. *Journal of applied physics*, 102, 034306.
- Chan, K., Aspanut, Z., Goh, B., Muhamad, M. R., & Rahman, S. A. (2011). Formation of gold nanoparticles in silicon suboxide films prepared by plasma enhanced chemical vapour deposition. *Thin solid films*.
- Choi, W., Choo, C., & Lu, Y. (1996). Electrical characterization of rapid thermal annealed radio frequency sputtered silicon oxide films. *Journal of applied physics*, 80(10), 5837-5842.
- Fu, G., Cai, W., Kan, C., Li, C., & Zhang, L. (2003). Controllable optical properties of Au/SiO₂ nanocomposite induced by ultrasonic irradiation and thermal annealing. *Applied physics letters*, 83, 36.
- Garcia-Serrano, J., Galindo, A., & Pal, U. (2004). Au-Al₂O₃ nanocomposites: XPS and FTIR spectroscopic studies. *Solar energy materials and solar cells*, 82(1-2), 291-298.
- Jung, K. H., Yoon, J. W., Koshizaki, N., & Kwon, Y. S. (2008). Fabrication and characterization of Au/SiO₂ nanocomposite films grown by radio-frequency cosputtering. *Current Applied Physics*, 8(6), 761-765.
- Ko, H. Y. Y., Mizuhata, M., Kajinami, A., & Deki, S. (2005). The dispersion of Au nanoparticles in SiO₂/TiO₂ layered films by the liquid phase deposition (LPD) method. *Thin solid films*, 491(1), 86-90.
- Pal, U., Almanza, E. A., Cuchillo, O. V., Koshizaki, N., Sasaki, T., & Terauchi, S. (2001). Preparation of Au/ZnO nanocomposites by radio frequency co-sputtering. *Solar energy materials and solar cells*, 70(3), 363-368.
- Ruffino, F., Bongiorno, C., Giannazzo, F., Roccaforte, F., Raineri, V., & Grimaldi, M. (2007). Effect of surrounding environment on atomic structure and equilibrium shape of growing nanocrystals: gold in/on SiO₂. *Nanoscale Research Letters*, 2(5), 240-247.
- Sangpour, P., Akhavan, O., Moshfegh, A., & Roozbehi, M. (2007). Formation of gold nanoparticles in heat-treated reactive co-sputtered Au-SiO₂ thin films. *Applied Surface Science*, 254(1), 286-290.
- Scalisi, A., Compagnini, G., D'Urso, L., & Puglisi, O. (2004). Nonlinear optical activity in Ag-SiO₂ nanocomposite thin films with different silver concentration. *Applied Surface Science*, 226(1-3), 237-241.
- Severi, M., Mattei, G., Dori, L., Maccagnani, P., Baldini, G., & Pizzochero, G. (1992). Electrical properties of thin SiO₂ films nitrided in N₂O by rapid thermal processing. *Microelectronic Engineering*, 19(1-4), 657-660.
- Su, X., Li, M., Zhou, Z., Zhai, Y., Fu, Q., Huang, C., . . . Hao, Z. (2008). Microstructure and multiphoton luminescence of Au nanocrystals prepared by using glancing deposition method. *Journal of Luminescence*, 128(4), 642-646.
- Tsuji, H., Arai, N., Ueno, K., Matsumoto, T., Gotoh, N., Adachi, K., . Ishikawa, J. (2006). Formation of mono-layered gold nanoparticles in shallow depth of SiO₂ thin film by low-energy negative-ion implantation. *Nuclear Instruments and Methods in Physics Research Section B: Beam Interactions with Materials and Atoms*, 242(1), 125-128.
- Xu, J., & Perry, C. C. (2007). A novel approach to Au@SiO₂ core-shell spheres. *Journal of Non-Crystalline Solids*, 353(11-12), 1212-1215.
- Yu, J., & Lu, Y. (2000). Effects of rapid thermal annealing on ripple growth in excimer laser-irradiated silicon-dioxide/silicon substrates. *Applied Surface Science*, 154, 670-674.
- Zhuo, B., Li, Y., Teng, S., & Yang, A. (2010). Fabrication and characterization of Au/SiO₂ nanocomposite films. *Applied Surface Science*, 256(10), 3305-3308.